# Syntheses of Two Co(II) and Ni(II) Complexes with 2-(1*H*-Imidazolyl-1-methyl)-1*H*-benzimidazole and 1,4-Benzenedicarboxylate Ligands and Their Effect on Cardiac Fibroblasts Proliferation

Ying Wang[a], Shuxun Yan[b], Yanzhou Zhang[c], Lina Sun[a], and Zihan Wei[a]

[a] Department of Geriatrics, The First Affiliated Hospital, Zhengzhou University, Zhengzhou 450001, P. R. China

[b] Department of Endocrinology and Metabolism, The First Affiliated Hospital, Henan College of Traditional Chinese Medicine, Zhengzhou, 450008, P. R. China

[c] Department of Cardiology, The First Affiliated Hospital, Zhengzhou University, Zhengzhou 450001, P. R. China

Reprint requests to Prof. Ying Wang. E-mail: wangying6662001@163.com

*Z. Naturforsch.* **2013**, *68b*, 1225 – 1232 / DOI: 10.5560/ZNB.2013-3151
Received May 14, 2013

Two new isostructural complexes based on 2-(1*H*-imidazolyl-1-methyl)-1*H*-benzimidazole (imb) and di-anionic 1,4-benzenedicarboxylate (bdic), namely, $\{[Co(bdic)(imb)_2(H_2O)_2]\cdot 2H_2O\}_n$ (**1**) and $\{[Ni(bdic)(imb)_2(H_2O)_2]\cdot 2H_2O\}_n$ (**2**), have been synthesized and characterized by single-crystal X-ray diffraction. Both complexes possess a chain structure with the di-anionic bdic groups bridging the metal ions. The imb ligands coordinate the metal ions in a monodentate mode at two sides of the main chain. These chains are further packed into 3D networks through five kinds of hydrogen bonds. The *in vitro* effect of **1** and **2** on cultured cardiac fibroblasts (CF) proliferation in the presence or absence of excessive angiotensin II (AngII) have been investigated by a flow cytometric assay. The results have indicated that both complexes have no obvious effect on the cell cycle distribution of CF, but they can suppress the CF proliferation induced by AngII.

*Key words:* Co(II) and Ni(II) Complexes, 2-(1*H*-Imidazolyl-1-methyl)-1*H*-benzimidazole, 1,4-Benzenedicarboxylate, Cardiac Fibroblast, Proliferation

## Introduction

Transition metal complexes with intriguing structures have received great attention due to their interesting properties and potential applications in ion exchange, molecular recognition and separation, heterogeneous catalysis, gas sorption and storage, drug delivery and medical imaging, and magnetic and porous materials [1 – 11]. However the exploration of synthetic strategies and routines is still a long-term challenge since the structure of the resultant complexes is influenced by various factors such as the metal ions and their coordinating possibilities, the coordination behavior and the multifunctionality of the ligands, the metal-to-ligand ratio, the nature of the counteranions, the reaction temperature, the pH values, and the solvent of recrystallization [12 – 15]. Among those factors mentioned above, the selection of the organic ligand plays an important role in the construction of complexes because these are the organic units that serve to coordinate to the metal centers and pass on the structural information expressed in metal coordination preferences throughout the extended structure. *N*-Heterocyclic compounds like imidazole, triazole, tetrazole, benzimidazole, benzotriazole, pyridine, pyrazine, and piperazine and their derivatives are extensively used as ligands to construct complexes due to their strong coordination ability and diversities of the coordination modes [16 – 23]. Furthermore, imidazole derivatives such as AICAR (AICAR = amino-imidazole-4-carboxamide-1-$\beta$-ribofuranoside) can activate AMPK (AMPK = AMP-activated kinase) in rat cardiac fibroblasts and increase AngII-induced (AngII = angiotensin II) extracellular signal-regulated kinase 1/2 phosphorylation and activity. AICAR can also increase AngII-induced c-fos mRNA expression in the cells [24]. Benzimidazole derivatives such as 4,5-dihydro-6-[2-(4-hydroxyphenyl)-1*H*-benzimidazole-5-yl]-5-methyl-3(2*H*)-pyridazinone, an active metabolite of pimobendan, has a positive inotropic ef-

fect partly due to an increase in myofibrillar $Ca^{2+}$ sensitivity that is exerted *via* cross talk with a signal transduction pathway that involves cAMP in Canine Ventricular Myocardium [25].

The aforementioned ideas prompted us to employ an imidazole derivative, 2-(1*H*-imidazolyl-1-methyl)-1*H*-benzimidazole (imb), as ligand to self-assemble with Co(II) or Ni(II) salts in the presence of 1,4-benzenedicarboxylic acid ($H_2$bdc). In this work, we present two new isostructural 1D complexes, $\{[Co(bdic)(imb)_2(H_2O)_2]\cdot 2H_2O\}_n$ (**1**) and $\{[Ni(bdic)(imb)_2(H_2O)_2]\cdot 2H_2O\}_n$ (**2**), and evaluate their effects on cultured cardiac fibroblasts (CF) proliferation *in vitro* by a flow cytometric assay in the presence or absence of excessive AngII.

## Experimental Section

The ligand 2-(1*H*-imidazolyl-1-methyl)-1*H*-benzimidazole (imb) was synthesized according to the literature method [26, 27]. All chemicals were commercially available and used without purification. IR data were recorded on a Bruker Tensor 27 spectrophotometer with KBr pellets from 400 – 4000 $cm^{-1}$. Elemental analyses were carried out on a Flash EA 1112 elemental analyzer. PXRD patterns were recorded using Cu$K_{\alpha 1}$ radiation on a PANalytical X'Pert PRO diffractometer. Gel permeation chromatography (GPC) analyses were carried out with Agilent 1100 series equipped with a RI-G1362A RI detector and a PL gel Mixed-C column using DMSO as the mobile phase at a flow rate of 1.0 mL $min^{-1}$. Molecular weights and molecular weight distributions were estimated on the basis of the calibration curve obtained by polystyrene standards.

*Synthesis of $\{[Co(bdic)(imb)_2(H_2O)_2]\cdot 2H_2O\}_n$ (**1**)*

A mixture of $CoCl_2\cdot 6H_2O$ (0.05 mmol), imb (0.1 mmol), $H_2$bdic (0.05 mmol), water (8 mL), and DMF (1 mL) was placed in a 25 mL Teflon-lined stainless-steel vessel and heated at 353 K for 3 d. After the mixture had been cooled to room temperature at a rate of 10 °C·$h^{-1}$, red crystals of **1** suitable for X-ray diffraction were obtained. Yield: 51 % based on Co. – Anal. for $C_{30}H_{32}CoN_8O_8$ (691.57): calcd. C 52.10, H 4.66, N 16.20; found C 52.43, H 4.39, N 15.96. – FT-IR (KBr, $cm^{-1}$): $\nu$ = 3460 (s), 3124 (s), 1665 (m), 1574 (s), 1539 (m), 1520 (s), 1444 (s), 1377 (s), 1333 (s), 1275 (s), 1109 (m), 1089 (s), 832 (s), 759 (s), 744 (s), 658 (s).

*Synthesis of $\{[Ni(bdic)(imb)_2(H_2O)_2]\cdot 2H_2O\}_n$ (**2**)*

The preparation of **2** was similar to that of **1** except that $NiCl_2\cdot 6H_2O$ (0.05 mmol) was used instead of $CoCl_2\cdot 6H_2O$. Green crystals of **2** were obtained. Yield: 43 % based on Ni. – Anal. for $C_{30}H_{32}N_8NiO_8$ (691.35): calcd. C 52.12, H 4.67, N 16.21; found C 52.39, H 4.43, N 16.01. – FT-IR (KBr, $cm^{-1}$): $\nu$ = 3464 (s), 3125 (s), 1665 (m), 1576 (s), 1539 (m), 1521 (s), 1444 (s), 1378 (s), 1333 (s), 1275 (s), 1109 (m), 1090 (s), 832 (s), 760 (s), 743 (s), 660 (s).

*Crystal structure determinations*

Single crystals of complexes **1** and **2** were attached to a thin glass fiber. Crystal structure determination by X-ray diffraction was performed on a Rigaku Saturn 724 CCD area detector with a graphite monochromator for the X-ray source (Mo$K_\alpha$ radiation, $\lambda$ = 0.71073 Å) operating at 50 kV and 40 mA. The data were collected by an $\omega$ scan mode at a temperature of 293(2) K, the crystal-to-detector distance was 45 mm. An empirical absorption correction was applied. The data were corrected for Lorentz and polarization effects. The structures were solved by Direct Methods, completed by difference Fourier syntheses and refined by full-matrix least-squares techniques based on $F^2$, using the programs SHELXS/L-97, respectively [28]. All non-hydrogen atoms were refined anisotropically. The hydrogen atoms of the ligands were positioned geometrically and refined using a riding model. The hydrogen atoms of the water molecules were found at reasonable positions in difference Fourier maps and located there. All the hydrogen atoms were included in the final refinement. Crystal data and numbers pertinent to data collection and structure refinement parameters for both complexes are summarized in detail in Table 1. Selected bond lengths and bond angles are listed in Table 2. Hydrogen bonds are given in Table 3.

CCDC 900679(**1**) and 900680(**2**) contain the supplementary crystallographic data for this paper. These data can be obtained free of charge from The Cambridge Crystallographic Data Centre *via* www.ccdc.cam.ac.uk/data_request/cif.

*Cardiac fibroblast culture and identification*

Primary cultures of cardiac fibroblasts were prepared from hearts of neonatal Sprague-Dawley rats (1 – 2 days old) as previously described with minor modifications [29]. After dissociation from the heart tissue by trypsin and collagenase, cells were pre-plated into culture flacons at 37 °C for 30 min to remove the suspended cells. The majority of the adherent cells are fibroblasts. Cardiac fibroblasts were routinely grown in Dulbecco's modified Eagle medium (DMEM) supplemented with 10 % newborn calf serum (NCS), 100 U $mL^{-1}$ penicillin and 100 $\mu$g $mL^{-1}$ streptomycin. The cell culture was grown in a humidified 5 % $CO_2$ and 95 % air incubator at 37 °C with media replenishment every 3 d. When cells became confluent they were harvested with 0.25 % trypsin/ethylenediaminetetraacetic acid and replated (passaged) with a split of 1 : 3. The medium was changed every

Table 1. Crystal data and structure refinement data of complexes **1** and **2**.

| | **1** | **2** |
|---|---|---|
| Empirical formula | $C_{30}H_{32}CoN_8O_8$ | $C_{30}H_{32}N_8NiO_8$ |
| Formula weight | 691.57 | 691.35 |
| Temperature, K | 293(2) | 293(2) |
| Crystal size, mm$^3$ | $0.21 \times 0.12 \times 0.11$ | $0.23 \times 0.20 \times 0.16$ |
| Crystal system | triclinic | triclinic |
| Space group | $P\bar{1}$ | $P\bar{1}$ |
| $a$, Å | 7.8608(16) | 7.8700(16) |
| $b$, Å | 9.0242(18) | 9.0304(18) |
| $c$, Å | 11.394(2) | 11.323(2) |
| $\alpha$, deg | 86.82(3) | 87.46(3) |
| $\beta$, deg | 83.63(3) | 83.84(3) |
| $\gamma$, deg | 84.87(3) | 84.71(3) |
| Volume, Å$^3$ | 799.2(3) | 891.8(3) |
| $Z$ | 1 | 1 |
| Calculated density, g cm$^{-3}$ | 1.44 | 1.44 |
| Absorption coefficient, mm$^{-1}$ | 0.6 | 0.7 |
| $F(000)$, e | 359 | 360 |
| $2\theta$ range data collection, deg | 1.80 – 51.00 | 2.61 – 55.68 |
| $hkl$ range | $\pm 9, \pm 10, \pm 13$ | $\pm 10, -11 \rightarrow 10, \pm 14$ |
| Refl. collected/unique/$R_{int}$ | 5535/2836/0.0266 | 9915/3754/0.0299 |
| Data/ref. parameters | 2836/214 | 3754/214 |
| Final $R1/wR2$ [$I > 2\,\sigma(I)$] | 0.0474/0.1163 | 0.0465/0.0970 |
| Final$R1/wR2$ (all data) | 0.0578/0.1324 | 0.0522/0.1002 |
| Goodness-of-fit on ($F^2$) | 1.191 | 1.076 |
| $\Delta\rho_{fin}$ (max/min), e Å$^{-3}$ | 0.29/−0.44 | 0.25/−0.33 |

Table 2. Selected bond lengths (Å) and angles (deg) for complexes **1** and **2**[a].

| Complex **1** | | Complex **2** | |
|---|---|---|---|
| Co1–O1 | 2.104(2) | Ni1–O1 | 2.0612(14) |
| Co1–O3 | 2.105(2) | Ni1–O3 | 2.0864(16) |
| Co1–N1 | 2.120(3) | Ni1–N1 | 2.0773(18) |
| O1–Co1–O1$^{\#1}$ | 180.0 | O1–Ni1–O1$^{\#1}$ | 180.0 |
| O1–Co1–O3$^{\#1}$ | 93.64(9) | O1–Ni1–O3$^{\#1}$ | 93.87(7) |
| O1–Co1–O3 | 86.36(9) | O1–Ni1–O3 | 86.13(7) |
| O3$^{\#1}$–Co1–O3 | 180.0 | O3$^{\#1}$–Ni1–O3 | 180.0 |
| O1–Co1–N1$^{\#1}$ | 90.67(10) | O1–Ni1–N1$^{\#1}$ | 90.41(7) |
| O3–Co1–N1$^{\#1}$ | 91.71(10) | O3–Ni1–N1$^{\#1}$ | 92.20(7) |
| O1–Co1–N1 | 89.33(10) | O1–Ni1–N1 | 89.59(7) |
| O3–Co1–N1 | 88.29(10) | O3–Ni1–N1 | 87.80(7) |
| N1$^{\#1}$–Co1–N1 | 180.0 | N1$^{\#1}$–Ni1–N1 | 180.0 |

[a] Symmetry transformations used to generate equivalent atoms: **1**: $^{\#1}$ $-x+2, -y+1, -z$; **2**: $^{\#1}$ $-x+1, -y+2, -z+1$.

Table 3. Hydrogen bonds of complexes **1** and **2**[a].

| D–H···A | $d$(D–H) (Å) | $d$(H···A) (Å) | $d$(D···A) (Å) | (D–H···A) (deg) |
|---|---|---|---|---|
| | | Complex **1** | | |
| O3–H2W···O4 | 0.85 | 1.87 | 2.703(4) | 167.9 |
| O3–H1W···O2$^{\#1}$ | 0.85 | 1.98 | 2.720(3) | 145.3 |
| N4–H4C···O2$^{\#3}$ | 0.86 | 1.92 | 2.737(4) | 158.9 |
| O4–H3W···O2$^{\#4}$ | 0.85 | 1.95 | 2.787(4) | 167.9 |
| O4–H4W···N3$^{\#4}$ | 0.85 | 1.98 | 2.814(4) | 167.2 |
| | | Complex **2** | | |
| O3–H2W···O4 | 0.85 | 1.88 | 2.721(2) | 169.1 |
| O3–H1W···O2$^{\#1}$ | 0.85 | 1.96 | 2.698(2) | 143.8 |
| N4–H4C···O2$^{\#3}$ | 0.86 | 1.92 | 2.739(3) | 158.7 |
| O4–H3W···O2$^{\#4}$ | 0.85 | 1.95 | 2.795(2) | 170.3 |
| O4–H4W···N3$^{\#4}$ | 0.85 | 1.99 | 2.820(3) | 167.2 |

[a] Symmetry transformations used to generate equivalent atoms: **1**: $^{\#1}$ $-x+2, -y+1, -z$; $^{\#3}$ $x, y+1, z$; $^{\#4}$ $x-1, y, z$; **2**: $^{\#1}$ $-x+1, -y+2, -z+1$; $^{\#3}$ $x, y-1, z$; $^{\#4}$ $x+1, y, z$.

2 d. Cells in passage three and four were used in all experiments. Cardiac fibroblasts purity was assessed by morphological observation under an inverted-phase contrast microscope and immunocytochemistry by using the antibody for vimentin. The culture contained more than 95 % fibroblasts.

*Preparation of stock solutions of complexes **1** and **2***

Complex **1** (172.89 mg) or **2** (172.84 mg) was weighed accurately and dissolved in 10 mL DMSO. Then 50 mL DMEM was added. The resulting solution was transferred to a 250 mL volumetric flask and diluted with DMEM. The concentration of the prepared stock solution was $1.0 \times 10^{-3}$ mol·L$^{-1}$ (in terms of structural unit). The dilution series were prepared by serial dilution of the stock solution with DMEM in 50 mL volumetric flasks.

*Cell viability assay*

Cell viability was determined using the MTT assay (MTT = 3-(4,5)-dimethylthiazo(-2-y1)-3,5-di-phenyltetraz-

oliumbromide). Briefly, the cells were collected and resuspended in DMEM at $4 \times 10^4$ cells per mL, and 100 $\mu$L aliquots were added to each well of 96-well flat-bottomed microtiter plates, followed by addition of 100 $\mu$L of the solution of the complex **1** or **2**. Three replicate wells were used for each data point in the experiments. After incubation for the indicated intervals, 20 $\mu$L of MTT (5 mg mL$^{-1}$ in PBS, PBS = phosphate buffer saline) solution was added to each well, and plates were then incubated for 4 h at 37 °C. The medium with MTT was removed from the wells. Intracellular formazan crystals were dissolved by adding 150 $\mu$L of DMSO to each well, and the plates were shaken for 10 min. The absorbance was read at 490 nm with a microplate reader (Thermo). From this MTT assay, we found an appropriate concentration (for complex **1** or **2**) which has no toxic effect on cardiac fibroblasts.

*Cell cycle assay*

The cells were collected and resuspended in DMEM with 10 % serum at $4 \times 10^4$ cells per mL, and 2 mL were added to each well of 6-well flat-bottomed microtiter plates. The cell culture was grown in a humidified 5 % $CO_2$ and 95 % air incubator at 37 °C for 24 h. After the cells became confluent, DMEM with serum was removed from the wells, and serum-free DMEM was added. Then cardiac fibroblasts in the wells were treated with complexes **1** and **2** in the presence or absence of excessive AngII (groups were listed in detail in Tables 4 and 5) for 24 h, harvested, washed in cold PBS (pH = 7.4), and fixed with 70 % (*v*/*v*) ethanol at −20 °C for 30 min. After the ethanol was removed, the cells were incubated with PBS containing RNase (172 mU L$^{-1}$) at 37 °C for 30 min, then stained for 30 min with 0.005 % propidium iodide. Fluorescence was measured with a flow cytometer (Coulter Epics-XL-MCL, USA). Results represented a minimum of 3000 cells assayed for each determination. The experiment was performed five times.

*Statistical analysis*

All results were expressed as mean and standard deviation (mean ± s. d.). The difference was analyzed for significance by one-way repeated-measures analysis of variance. A value of $P < 0.05$ was considered statistically significant.

## Results and Discussion

*IR spectroscopy of complexes **1** and **2***

In the IR spectra the absorption bands at 3460 cm$^{-1}$ for **1** and at 3464 cm$^{-1}$ for **2** are associated with the stretching vibrations of the hydroxyl groups, and absorption bands at 3124 cm$^{-1}$ for **1** and at 3125 cm$^{-1}$ for **2** attributed to Ar–H stretching vibrations [30]. Furthermore, the absorption bands at 1574, 1520, and 1444 cm$^{-1}$ for **1** and at 1576, 1521 and 1444 cm$^{-1}$ for **2** originate from C=C and C=N stretching vibrations [31, 32]. The band at 1333 cm$^{-1}$ for **1** and **2** is the results of C–N stretching vibrations. The absorption bands at 744 cm$^{-1}$ for **1** and at 743 cm$^{-1}$ for **2** can be assigned to characteristic stretching vibrations of *o*-phenylene [33]. The absorption band at 832 cm$^{-1}$ for **1** and **2** corresponds to the stretching vibrations of *t*-phenylene [34]. Separations ($\Delta$) between $\nu_a$(COO) and $\nu_s$(COO) are different for the unidentate, chelating (bidentate) and bridging complexes. In **1**, the separation $\Delta$ is 288 cm$^{-1}$ (1665 *vs.* 1377 cm$^{-1}$), and the carboxylate groups are thus coordinate to Co(II) ions in a unidentate fashion. In **2**, the carboxylate groups exhibit $\nu_a$(COO) and $\nu_s$(COO) at 1665 and 1378 cm$^{-1}$ ($\Delta = 287$ cm$^{-1}$), also comparable to those of monodentate carboxylate groups. The above analyses are confirmed by the results of the structure determinations.

*Description of the cyrstal and molecular structures*

Single-crystal X-ray analysis has revealed that structures **1** and **2** are triclinic and crystallize in the space group $P\bar{1}$ with $Z = 1$, *i. e.* the complexes exhibit crystallographic inversion symmetry. Complexes **1** and **2** are isostructural with only slight differences in bond lengths and angles (see Tables 1 and 2). Therefore only the structure of **1** is discussed in detail here (Fig. 1). The respective plots of complex **2** are given in the Supporting Information available online (see note at the end of the paper for availability). There is one half Co(II) ion, one half 1,4-benzenedicarboxylate anion, one imb ligand, one coordinated water molecule and one uncoordinated water molecule in the asymmetric unit of complex **1**. As shown in Fig. 1a, the Co(II) ion is hexacoordinated in a slightly distorted octahedral geometry. Four O atoms (O1, O1$^{\#1}$, O3, O3$^{\#1}$) from two symmetry-related 1,4-benzenedicarboxylate anions and two symmetry-related water molecules, respectively, occupy the equatorial positions, and two nitrogen atoms (N1, N1$^{\#1}$) from two symmetry-related imb ligands are located in the apical positions (the N1–Co1–N1$^{\#1}$ bond angle therefore is strictly 180.0). The Co–O distances of 2.104(2) and 2.105(2) Å and the Co–N distance of 2.120(3) Å are close to those in other Co(II) compounds, *e. g.* {[Co(L)(phen)($H_2O$)]·MeOH} (L = 5-

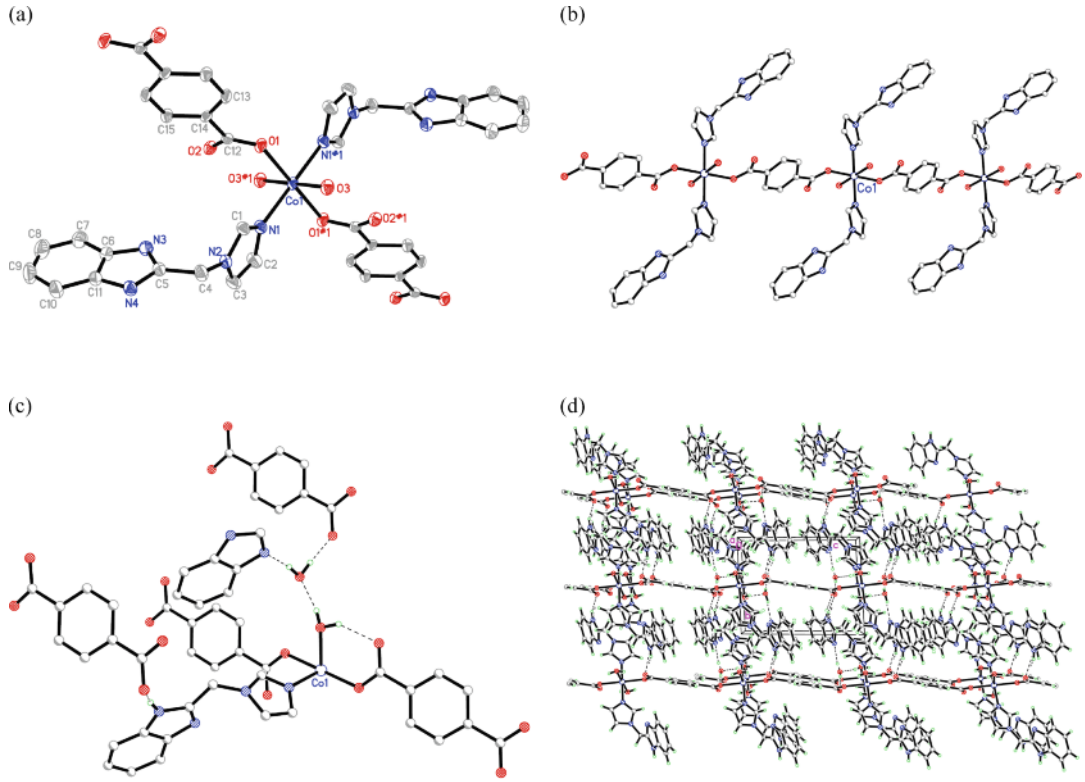


Fig. 1. (a) Coordination environment of the Co(II) centers in complex **1** with the atom numbering scheme. Uncoordinated water molecules and hydrogen atoms are omitted for clarity. (b) View of the chain structure of complex **1**. (c) View of hydrogen bonds in complex **1**. (d) 3D structure of complex **1** in the solid state supported by hydrogen bonds.

ferrocenyl-1,3-benzenedicarboxylic acid, phen = 1,10-phenanthroline) [35] and $[Co(OOC(CH_2)_4Fc)_2(4,4'\text{-bipy})(H_2O)_2]_n$ (Fc = $(\eta^5\text{-}C_5H_5)Fe(\eta^5\text{-}C_5H_4)$, bbbm = 1,1′-(1,4-butanediyl)bis-1*H*-benzimidazole) [36].

In complex **1**, the $H_2$bidc ligand is completely deprotonated, and the centroid of the 1,4-benzenedicarboxylate anion is located on a center of inversion. As shown in Fig. 1b, each di-anionic ligand bdic bridges two Co(II) ions to form a chain *via* Co–O bonds, and all of the carboxylate groups coordinate to the Co(II) centers in the monodentate mode. The distance of Co(II)···Co(II) bridged by the bdic ligand is 11.394 Å. Imb ligands coordinate to the Co(II) centers in monodentate mode at two sides of the main chain. The dihedral angle between the imidazol and benzimidazol planes is 86.2°. All benzimidazole rings on the same side are parallel, and the distance between the neighboring benzimidazole rings is 8.753 Å. As shown in Fig. 1c, there are five kinds of hydrogen bonds in complex **1**: (a) coordinated/uncoordinated water molecules (O···O distance: 2.703(4) Å); (b) coordinated water molecules/carboxyl O atoms (O···O distance: 2.720(3) Å); (c) uncoordinated water molecules/carboxyl O atoms (O···O distance: 2.787(4) Å); (d) uncoordinated water molecules/benzimidazole N atoms (O···N distance: 2.814(4) Å); (e) benzimidazole/carboxyl O atoms (N···O distance: 2.737(4) Å). The chains are thus connected by the above O–H···O, O–H···N and N–H···O hydrogen bonds leading to a 3D structure (Fig. 1d).

*XRD patterns*

To confirm the phase purity of the two complexes, PXRD patterns were recorded for **1** and **2**, and they were compared to the corresponding simulated ones as calculated on the basis of the single-crystal diffraction data (Fig. 2), indicating a pure phase of each bulk sample within the limits of the powder diffraction experiment. In addition, by comparing the PXRD patterns

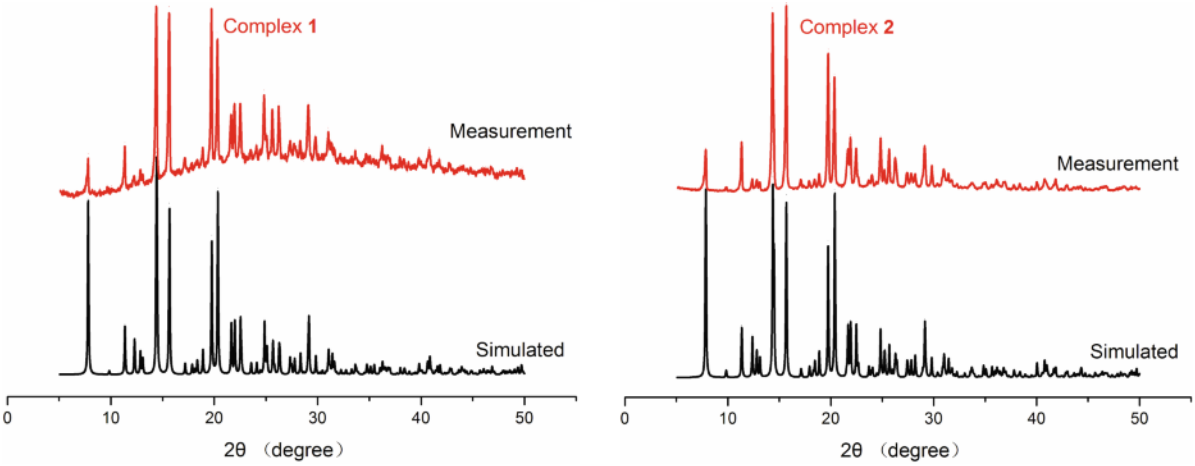


Fig. 2. The PXRD patterns of complexes **1** and **2** at room temperature; simulated patterns are generated from single-crystal diffraction data.

of complexes **1** and **2**, we can also confirm that complexes **1** and **2** are isostructural. This is consistent with the results of the single-crystal X-ray diffraction.

*The effects of complexes **1** and **2** on cultured cardiac fibroblasts proliferation*

Being a major pathogenic factor, AngII can induce cardiac fibroblasts proliferation, increase collagen synthesis, produce myocardial fibrosis, and play a very important role in the activation and the development of various cardiovascular diseases, such as chronic heart failure, myocardial infarction, arrhythmia and others [37]. Many studies have confirmed that many drugs can protect myocardium through inhibition of the biological effect of AngII. According to reports in the literature [24], the imidazole derivative AICAR can inhibit the biological effect of AngII and protect myocardium. Complexes **1** and **2** also contain imidazole groups. So we investigated the effects of both complexes on cultured cardiac fibroblasts proliferation. Through the cell viability assay, we found that there is no cytotoxicity when the concentration of complex **1** or **2** is $1.0 \times 10^{-5}$ mol L$^{-1}$. In order to elucidate the effects of complexes **1** and **2** on cultured cardiac fibroblasts proliferation *in vitro*, the cell cycle distribution was analyzed by a flow cytometric assay in the presence or absence of excessive AngII. First, we investigated the effects of complexes **1** and **2** on the cell cycle distribution of cultured cardiac fibroblasts in the absence of exogenous stimulation. CF incubated with serum-free DMEM served as control group. In groups 1 and 2, CFs were incubated with serum-free DMEM containing complex **1** and **2**, respectively. The cells were harvested 24 h later. After a series of treatment, the cells cycle distribution was analyzed by flow cytometry using the SPSS 170 software. As shown in Table 4, the percentages of CFs in the $G_0/G_1$, $G_2/M$ and S phases have no significant difference in groups 1 and 2 compared with the control group ($P > 0.05$, $G_0$ is dormancy stage, $G_1$ is the first gap, $G_2$ is the second gap, M is mitosis phase, and S is synthesis phase). The results show that both complexes do not interfere with the cell cycle distribution of CF determined by flow cytometry compared with the control group. Second, we investigated the effects of the two complexes on the cell cycle distribution in the presence of AngII. CF incubated with serum-free DMEM also served as control group. CF incubated with serum-free DMEM containing AngII, AngII and complex **1**, AngII and complex **2** were defined as groups 1, 2 and 3, respectively. The cells were harvested 24 h later. As depicted in Table 5, there were significantly decreased $G_0/G_1$ and $G_2/M$ phase distributions, and an increased S phase distribution in group 1 compared to the control group ($P < 0.05$). That indicates that AngII can significantly increase cardiac fibroblasts proliferation, similar to that reported in the literature [38]. The addition of complexes **1** or **2** to the cells stimulated with AngII resulted in increased rates of cells at $G_0/G_1$ and $G_2/M$ phase distributions and decreased rates of cells at S phase compared to the group AngII alone ($P < 0.05$).

Table 4. The cell cycle analysis of the CF induced by complexes **1** and **2** for 24 h ($\bar{x} \pm s$).

| Groups | Components | $G_0/G_1$ | $G_2/M$ | S |
|---|---|---|---|---|
| Control group | DMEM (2 mL), CF (10 000 cells) | $69.59 \pm 1.76$ | $15.25 \pm 1.25$ | $15.14 \pm 1.14$ |
| Group 1 | DMEM (2 mL), CF (10 000 cells), complex **1** ($1.0 \times 10^{-5}$ mol L$^{-1}$) | $70.73 \pm 0.75$ | $11.70 \pm 0.82$ | $17.54 \pm 0.07$ |
| Group 2 | DMEM (2 mL), CF (10 000 cells), complex **2** ($1.0 \times 10^{-5}$ mol L$^{-1}$) | $68.57 \pm 1.54$ | $15.67 \pm 0.22$ | $15.51 \pm 1.31$ |

Table 5. The cell cycle analysis of the CF induced by Ang II and the complexes for 24 h ($\bar{x} \pm s$).

| Groups | Components | $G_0/G_1$ | $G_2/M$ | S |
|---|---|---|---|---|
| Control group | DMEM (2 mL), CF (10 000 cells) | $69.59 \pm 1.76$ | $15.25 \pm 1.25$ | $15.14 \pm 1.14$ |
| Group 1 | DMEM (2 mL), CF (10 000 cells), Ang II ($1.0 \times 10^{-6}$ mol L$^{-1}$) | $57.98 \pm 2.13$ | $9.44 \pm 3.16$ | $32.57 \pm 4.66$ |
| Group 2 | DMEM (2 mL), CF (10 000 cells), Ang II ($1.0 \times 10^{-6}$ mol L$^{-1}$), complex **1** ($1.0 \times 10^{-5}$ mol L$^{-1}$) | $66.56 \pm 2.44$ | $15.58 \pm 4.79$ | $17.86 \pm 4.01$ |
| Group 3 | DMEM (2 mL), CF (10 000 cells), Ang II ($1.0 \times 10^{-6}$ mol L$^{-1}$), complex **2** ($1.0 \times 10^{-5}$ mol L$^{-1}$) | $68.83 \pm 0.11$ | $14.77 \pm 0.49$ | $16.42 \pm 0.38$ |

There are only slight differences in effect between the two complexes ($P > 0.05$). These results suggest that both complexes can inhibit CF proliferation induced by AngII.

Furthermore, we determined the molecular weights of complexes **1** and **2** in DMSO solution. The results show that the average molecular weights (*Mn*) are 4828 for complex **1** and 4275 for complex **2**. The polydispersity indices (PDI) are 1.18 and 1.22 for complexes **1** and **2**, respectively. Thus we confirm that the skeletons of complexes **1** and **2** are intact in solution. So to some extent the properties of complexes **1** and **2** in solution can represent the properties of the crystals.

## Conclusion

Through the assembly of the *N*-heterocyclic ligand 2-(1*H*-imidazolyl-1-methyl)-1*H*-benzimidazole (imb) with Co(II) or Ni(II) salts in the presence of 1,4-benzenedicarboxylic acid ($H_2$bdic), two new isostructural 1D complexes $\{[Co(bdic)(imb)_2(H_2O)_2]\cdot 2H_2O\}_n$ (**1**) and $\{[Ni(bdic)(imb)_2(H_2O)_2]\cdot 2H_2O\}_n$ (**2**) were obtained. Their effects on cultured cardiac fibroblasts (CF) proliferation were studied by cell cycle analysis, and the results have shown that both complexes have no obvious effect on the CF cell cycle, but they can suppress the CF proliferation induced by AngII. We will continue to synthesize more complexes based on imb ligands and study their effects on cultured cardiac fibroblasts proliferation systemically.

*Supporting information*

Plots of the molecular and crystal strcutures of the Ni(II) complex **2** are given as Supporting Information available online (DOI: 10.5560/ZNB.2013-3151).

*Acknowledgement*

We gratefully acknowledge the financial support by the youth innovation fund of the first affiliated hospital of Zhengzhou University (no. 2011), Henan medical science and technology research program (no. 2011020038), Henan health science and technology innovation young talent project (no. 4099), the key project of science and technology of the Education Department of Henan province (no. 13A320436), the young backbone teachers in colleges and universities in Henan province project plan, Henan Province basic and frontier technology research projects, and the key laboratory of the first affiliated hospital of Zhengzhou University.

[1] M. Wriedt, A. A. Yakovenko, G. J. Halder, A. V. Prosvirin, K. R. Dunbar, H. C. Zhou, *J. Am. Chem. Soc.* **2013**, *135*, 4040.

[2] Z. Hao, S. Song, S. Su, X. Song, M. Zhu, S. Zhao, X. Meng, H. Zhang, *Cryst. Growth Des.* **2013**, *13*, 976.

[3] B. A. Blight, R. Guillet-Nicolas, F. Kleitz, R. Y. Wang, S. Wang, *Inorg. Chem.* **2013**, *52*, 1673.

[4] Y. Q. Lan, H. L. Jiang, S. L. Li, Q. Xu, *Adv. Mater.* **2011**, *23*, 5015.

[5] X. J. Gu, Z. H. Lu, H. L. Jiang, T. Akita, Q. Xu, *J. Am. Chem. Soc.* **2011**, *133*, 11822.
[6] K. P. Rao, M. Higuchi, J. Duan, S. Kitagawa, *Cryst. Growth Des.* **2013**, *13*, 981.
[7] J. W. Shin, J. M. Bae, C. Kim, K. S. Min, *Inorg. Chem.* **2013**, *52*, 2265.
[8] V. Percec, H. J. Sun, P. Leowanawat, M. Peterca, R. Graf, H. W. Spiess, X. Zeng, G. Ungar, P. A. Heiney, *J. Am. Chem. Soc.* **2013**, *135*, 4129.
[9] P. Z. Li, Y. Maeda, Q. Xu, *Chem. Commun.* **2011**, *47*, 8436.
[10] Y. Gong, P. G. Jiang, J. Li, T. Wu, J. H. Lin, *Cryst. Growth Des.* **2013**, *13*, 1059.
[11] T. Hirano, K. Uehara, S. Uchida, M. Hibino, K. Kamata, N. Mizuno, *Inorg. Chem.* **2013**, *52*, 2662.
[12] P. Zhang, D. S. Li, J. Zhao, Y. P. Wu, C. Li, K. Zou, J. Y. Lu, *J. Coord. Chem.* **2011**, *64*, 2329.
[13] R. B. Zhang, Z. J. Li, Y. Y. Qin, J. K. Cheng, J. Zhang, Y. G. Yao, *Inorg. Chem.* **2008**, *47*, 4861.
[14] M. O. Awaleh, A. Badia, F. Brisse, *Cryst. Growth Des.* **2006**, *6*, 2674.
[15] R. P. Feazell, C. E. Carson, K. K. Klausmeyer, *Inorg. Chem.* **2006**, *45*, 2635.
[16] C. H. Ke, G. R. Lin, B. C. Kuo, H. M. Lee, *Cryst. Growth Des.* **2012**, *12*, 3758.
[17] X. Zhu, X. Y. Wang, B. L. Li, J. Wang, S. Gao, *Polyhedron* **2012**, *31*, 77.
[18] G. H. Tao, D. A. Parrish, J. M. Shreeve, *Inorg. Chem.* **2012**, *51*, 5305.
[19] X. R. Meng, Y. L. Song, H. W. Hou, H. Y. Han, B. Xiao, Y. T. Fan, Y. Zhu, *Inorg. Chem.* **2004**, *43*, 3528.
[20] X. R. Meng, X. J. Wu, D. W. Li, H. W. Hou, Y. T. Fan, *Polyhedron* **2010**, *29*, 2619.
[21] H. L. Wu, J. K. Yuan, X. C. Huang, F. Kou, B. Liu, F. Jia, K. T. Wang, Y. Bai, *Inorg. Chim. Acta* **2012**, *390*, 12.
[22] C. D. Ene, A. Lungu, C. Mihailciuc, M. Hillebrand, C. Ruiz-Pérez, M. Andruh, *Polyhedron* **2012**, *31*, 539.
[23] A. Banisafar, D. P. Martin, J. S. Lucas, R. L. LaDuca, *Cryst. Growth Des.* **2011**, *11*, 1651.
[24] Y. Hattori, K. Akimoto, T. Nishikimi, H. Matsuoka, K. Kasai, *Hypertension* **2006**, *47*, 265.
[25] R. Takahashi, Y. Shimazaki, M. Endoh, *J. Pharmacol. Exp. Ther.* **2001**, *298*, 1060.
[26] A. R. Katritzky, M. Drewniak-Deyrup, X. F. Lan, *Heterocycl. Chem.* **1989**, *26*, 829.
[27] J. H. Burckhalter, V. C. Stephens, L. A. R. Hall, *J. Am. Chem. Soc.* **1952**, *74*, 3868.
[28] G. M. Sheldrick, *Acta Crystallogr.* **2008**, *A64*, 112.
[29] D. J. Autelitano, R. Ridings, L. Pipolo, W. G. Thomas, *Regul. Pept.* **2003**, *112*, 131.
[30] S. X. Yan, D. Zhao, T. Li, R. Wang, X. R. Meng, *J. Coord. Chem.* **2012**, *65*, 945.
[31] A. Majumder, V. Gramlich, G. M. Rosair, S. R. Batten, J. D. Masuda, M. S. E. Fallah, J. Ribas, J. P. Sutter, C. Desplanches, S. Mitra, *Cryst. Growth Des.* **2006**, *6*, 2355.
[32] G. H. Jin, Y. Yang, X. L. Zhou, X. R. Meng, *Z. Naturforsch.* **2012**, *67b*, 29.
[33] X. R. Meng, W. Zhou, Y. F. Qi, H. W. Hou, Y. T. Fan, *J. Organomet. Chem.* **2010**, *695*, 766.
[34] K. Nakamoto, *Infrared and Raman Spectra of Inorganic and Coordination Compounds*, Part B, 6th ed., John Wiley, Hoboken, NJ **2009**.
[35] X. Li, W. Liu, H. Y. Zhang, B. L. Wu, *J. Organomet. Chem.* **2008**, *693*, 3295.
[36] X. R. Meng, Y. Liu, H. W. Hou, Y. T. Fan, *J. Mol. Struct.* **2009**, *933*, 163.
[37] A. H. Siddiqui, R. A. Irani, W. Zhang, W. Wang, S. C. Blackwell R. E. Kellems, Y. Xia, *Hypertension* **2013**, *61*, 472.
[38] A. Simm, C. Diez, *Basic Res. Cardiol.* **1999**, *94*, 464.